

Structure and Nanocrystallites of Ni and NiO Three Dimensional Ordered Macromeshes

W.L. Zhou^a, L. Xu^a, A.A. Zakhidov^b, R.H. Baughman^b, and J.B. Wiley^a

^aAdvanced Materials Research Institute, Department of Chemistry, University of New Orleans, LA 70148

^bHoneywell Int., Corporate Technology, Morristown, NJ 07962

E-mail: wzhou@uno.edu

ABSTRACT

Three dimensional Ni and NiO inverse opal macromeshes were characterized by scanning electron microscope (SEM) and transmission electron microscope (TEM). The octahedral cubes of the macroporous Ni were found mostly grown as single crystals with stacking faults and microtwins. There was no preferential growth of these cubes as determined by selected area diffraction pattern (SADP). Some NiO nanocrystals with size of about 5 nm were formed on the surface of inverse Ni opal membrane during etching away of silica spheres. The oxidation of Ni mesh turned it into NiO macromesh with grain size of about 20 nm at 550°C. The nanocrystalline NiO mesh is suitable for further fabrication of three dimensional nanobeads. By annealing the meshes at 650°C, the NiO nanograins grew to a size of over 50 nm. This three dimensional ordered macroporous structure with higher temperature treatment is considered as stable and important for further application.

INTRODUCTION

Recently we reported on the use of inverse opals as the templates to generate three dimensionally ordered nanobeads from various functional materials such as metals [1,2]. Therefore it is important to study the structure and nanocrystallites in such inverse metal membranes to understand its growth mechanism for future application. The fabrication of macromeshes of metal and polymer have been reported by several groups [3-7]. The potential applications of these three dimensional macroporous structure will be in photonic, catalysis and magnetics. The detailed study of the nanostructure and nanocrystallites could possibly improve the fabrication of three dimensional free standing macromesh for various purposes.

EXPERIMENTAL

The opal template used here was composed of 290 nm silica spheres. The fabrication of macroporous Ni was done by electrochemical deposition, which was reported elsewhere [1]. The advantage of electrodeposition method is that one is able to control the filling depth by controlling the deposition time. Secondly it is easier to obtain homogeneous large scale free standing three dimensional macroporous structure for further application. Ni mesh was obtained by etching away silica beads using 2% HF. The NiO macromesh was obtained by slowly oxidizing the Ni mesh in open air by

heating to 550°C at 1°C/min. Scanning electron microscopy was performed using a JEOL 5410 SEM. Transmission electron microscopy investigation was carried out with a JEOL 2010 at 200kV. The TEM samples were prepared by putting small pieces of mesh on TEM copper grid and directly loaded in TEM for observation.

RESULTS AND DISCUSSION

As-deposited opal sample was broken into small pieces and directly put in SEM for observation. Figure 1a is a SEM cross-sectional micrograph of the sample near the electrode side (Au film side). The Ni appeared as ordered white dots on the opal surface and was also confirmed by electron energy dispersive (EDS) analysis. It seems that the Ni infiltration was a bit uneven at the top area as shown in figure 1b. The white ordered dots among the spherical silica beads are Ni metal. It was hard to estimate the Ni deposition thickness under SEM.

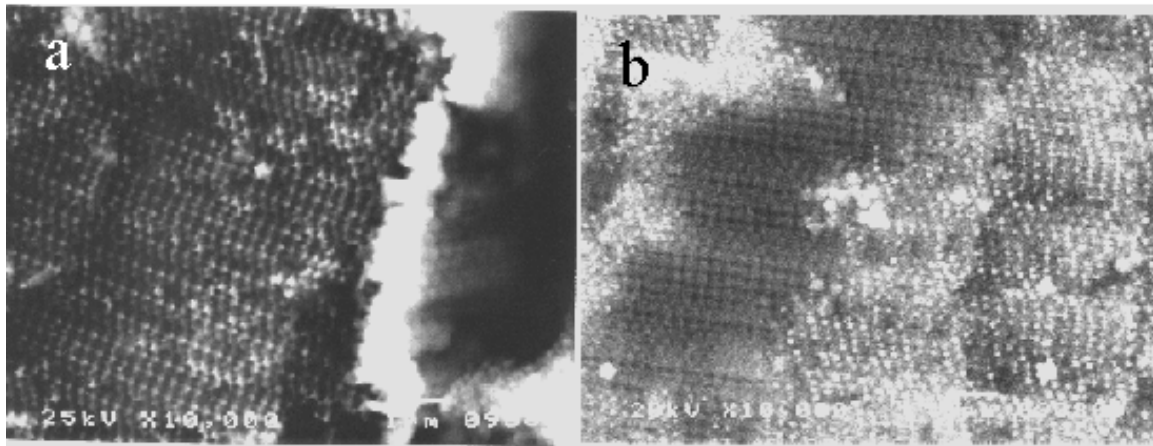


Figure 1. Cross-sectional SEM images of (a) nickel metal infiltrated near the Au film (b) nickel metal deposited at the top area of the opal.

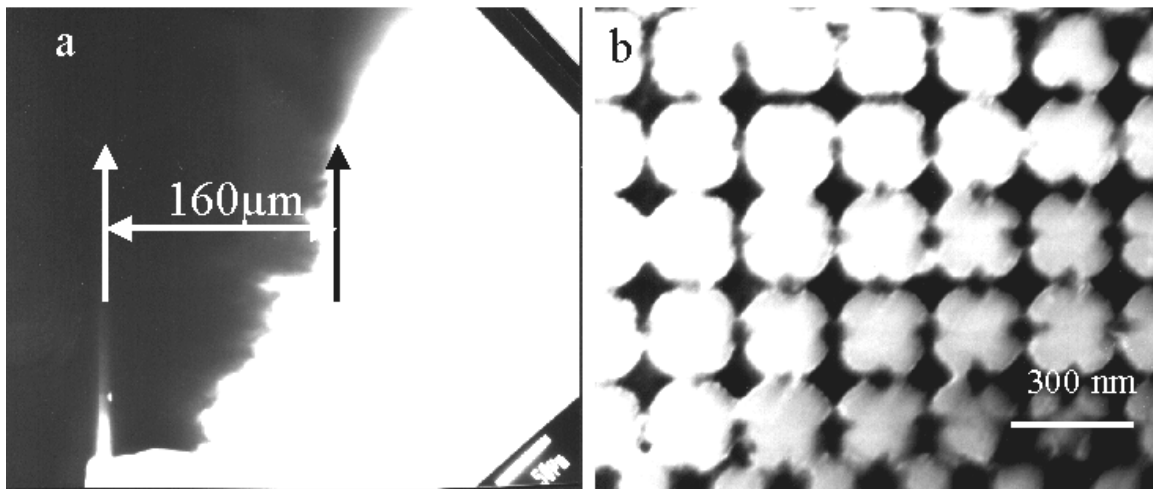


Figure 2. Cross-sectional TEM images of (a) thickness of infiltrated Ni in opal (b) the black nickel octahedral cubes infiltrated in the opal interstices.

In order to know the exact thickness of as-deposited Ni samples, a cross-sectional sample was prepared by gluing the sample between two silicon pallets and cutting into slices. The sample was then ground, polished and ion milled until transparency for electron beam. The thickness of the electrodeposited Ni could be clearly determined along the edge of the sample by TEM. In our case the thickness of the deposited Ni is around 160 nm as shown in figure 2a. Figure 2b is (001) monolayer opal with the Ni (black contrast) infiltrated in the opal interstices. By putting the metal-opal into 2% HF solution for about 24 hours, we could etch away the colloidal silica and obtain the free standing rigid inverse Ni macromesh. Figure 3a is a SEM image observed from [001] direction. The square features are essentially cubes with concave sides that arise from filling the octahedral sites in the close packed structure. Each cube is connected to eight other cubes through its vertices via tetrahedra [2]. We can also see the second layer Ni cubes through the first layer Ni pores. The inset is the higher resolution SEM image which clearly shows the connections of octahedral and tetrahedral nickel cubes forming rigid Ni membrane. By loading a small piece of the inverse Ni macromesh on a TEM copper grid, the two dimensional projection of Ni network can be seen as shown in figure 3b. Microtwins and stacking faults were found as shown in the left inset by

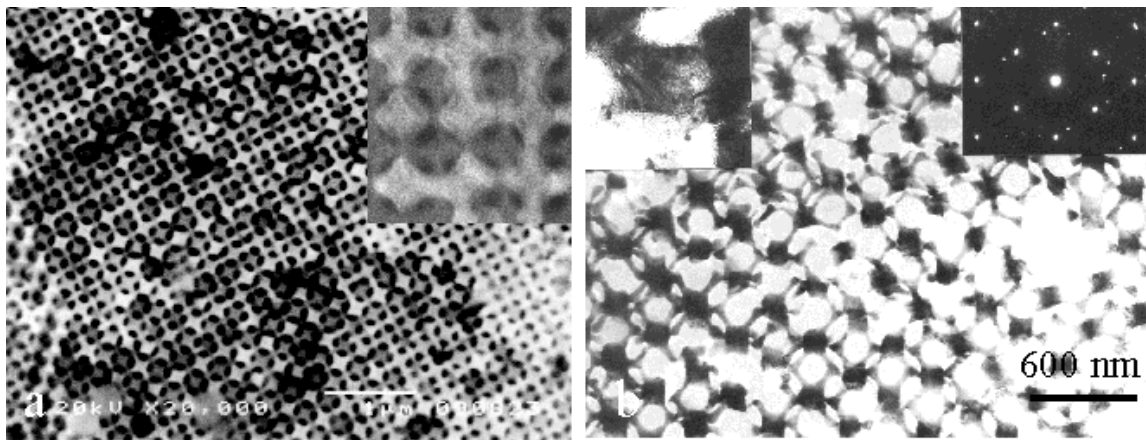


Figure 3 (a) (100) inverse nickel macroporous. The inset is the higher resolution of connections of octahedral and tetrahedral nickel cubes. (b) TEM micrograph of inverse Ni frame. The inset on the left is a single octahedral cube and the left is the SADP of the cube.

carefully investigating a single cube, which can be also determined from the $\langle 011 \rangle$ SADP as shown in the right side inset. The streaks and twin diffraction spots can be clearly seen. By doing SADPs of many nickel octahedra, we found that most of the octahedral cubes formed single crystals during the electrodeposition. The reason for forming such unique structure is that the octahedral interstices have bigger space and gave enough time for Ni cubes to crystallize and grow into homogeneous structure. The connections of the macromesh were composed of nanograins. The narrow space of connections and large silica surface provide a rapid quenching environment for forming Ni nanograins. Even though the single crystal octahedral Ni cubes were formed, it was hard to find any preferential growth of these nanocubes by doing SADP. The SADP

showed polycrystalline feature with homogenous diffraction rings. The nanograins of the connections were composed of Ni nanocrystallites with size ranging from 20-50 nm. Additionally, some small nanocrystals with size about 5 nm was often found sticking to the surface of the Ni membrane after etching away silica beads as shown in figure 4a. By doing EDS analysis, these nanoparticles were contained Ni and oxygen, which was confirmed as NiO nanocrystals by doing SADP. Figure 4b is the high resolution image of these nanocrystals. Similar phenomena was also observed by Blanford *et al.*[9]. When they removed the template in an oxygen containing atmosphere, any metal form

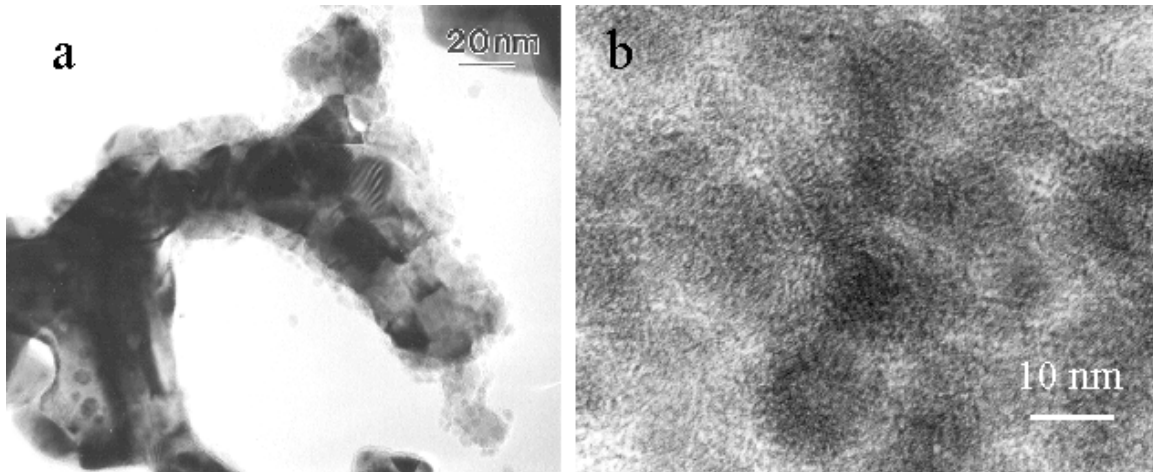


Figure 4 (a) some nanoparticles stick on the surface of the Ni macromesh. (b) HREM images of NiO nanocrystals.

was immediately oxidized forming metal oxide. In our case, when the silica beads were etched away, the fresh Ni surface was exposed to air and easily oxidized and formed NiO nanocrystals. In addition, the feature of Ni and NiO macromeshes are quite different from those prepared by chemical synthesis method reported by Yang *et al* [10]. In their samples Ni or NiO walls of macromeshes were composed of fused nanograins with size of about 50 nm and 6 nm, respectively. The NiO phase was found by them was hexagonal structure. In our case the nanocrystals of the NiO on the surface of the Ni membrane is of cubic structure with size about 5 nm.

By annealing the Ni membrane in air, the NiO semiconductor macromesh was obtained as shown in SEM image in figure 5a. The size of the pores became smaller due to the oxidation of Ni macromesh. The macromesh is quite uniform and good for further fabrication [2]. The annealing process turned the Ni membrane completely into a mesh consisted of NiO nanograins. Figure 5b is the (011) TEM image of the macromesh. All of the macromesh now was composed of fused NiO nanograins with an average diameter of 20 nm. The inset is the SADP of the NiO membrane with fcc structure. Further annealing of the NiO membrane at 650°C induced the NiO nanograins to grow bigger. TEM picture as shown in figure 6a shows that NiO nanograins grew into a size of 50-80 nm. By using the NiO macromesh as a template as shown in figure 6a, three dimensional ordered Au nanobeads were successfully fabricated. The higher temperature treatment made NiO membrane more stable for further application. Experiments are continuing for fabrication of metal nanobeads using NiO macromesh treated at 650°C.

CONCLUSIONS

Three dimensional Ni and NiO membrane prepared by electrodeposition were studied by SEM and TEM, respectively. The octahedral cubes of Ni membrane were grown mostly as single crystals with stacking faults and microtwins. The connections of the membrane were composed of Ni nanograins with a size of about 10-50 nm. Small nanocrystals with size of about 5 nm were found on the surface of Ni membrane after etching away silica beads. The fresh Ni macromesh is air sensitive. By annealing the Ni mesh at 550°C, the membrane completely turned into a macromesh fused by 20 nm NiO nanograins. The template is good for fabrication of three dimensional ordered metal nanobeads. By annealing the NiO macromesh at 650°C, the NiO nanograins grew into bigger nanograins with a size over 50 nm. This membrane has potential applications.

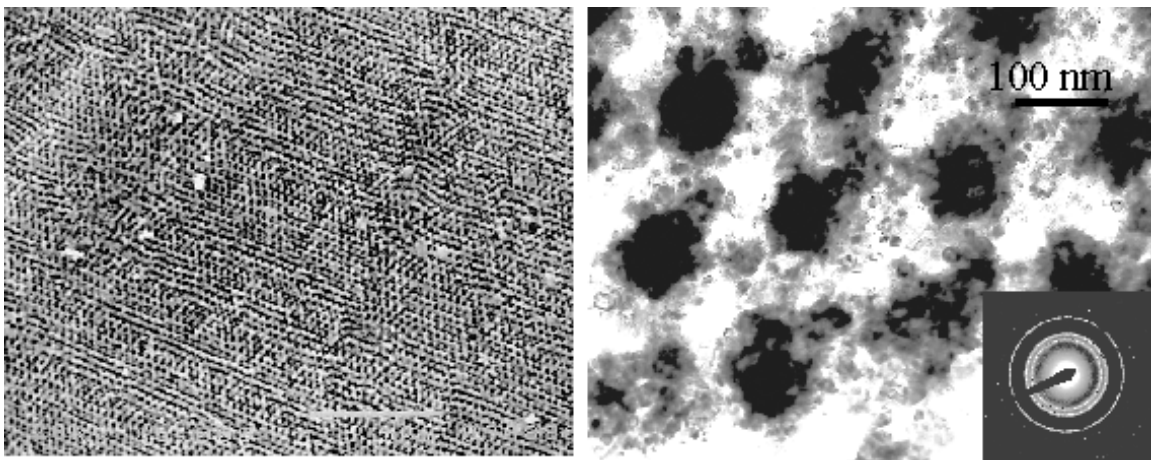


Figure 5 (a) SEM image of NiO macromesh after annealing Ni mesh at 550°C. (b) (011) TEM image of the NiO mesh composed of 20 nm nanograins. The inset is the SADP.

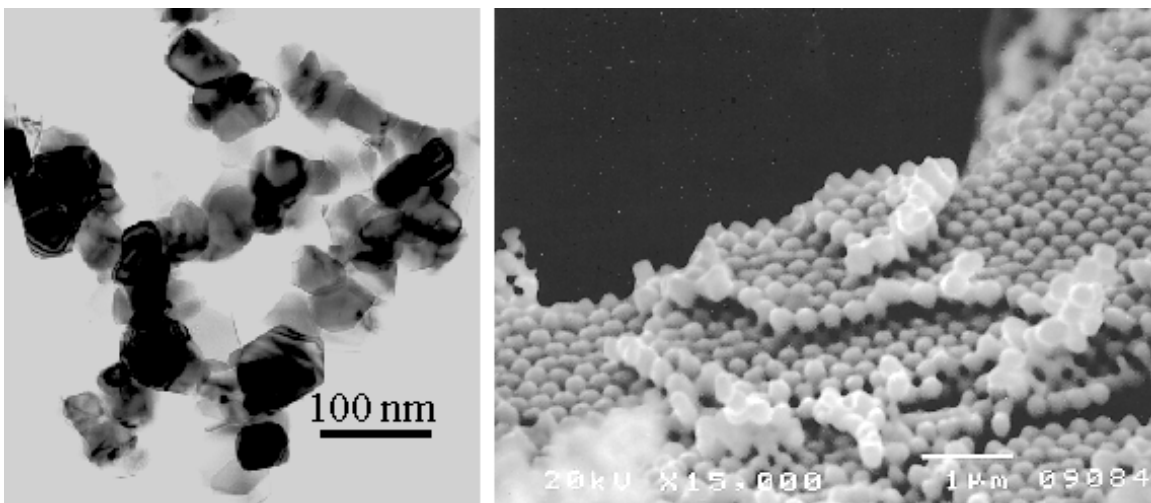


Figure 6 (a) 650°C heat treatment NiO membrane. (b) three dimensional ordered Au nanobeads.

ACKNOWLEDGMENTS

This work is supported by the Department of Defense (DARPA MDA 972-97-1-0003 and DAAB07-97-C-J036).

REFERENCES

1. L. Xu, W.L. Zhou, C. Frommen, R.H. Baughman, A.A. Zakhidov, L. Malkinski, J.-Q. Wang, and J.B. Wiley, *Chem. Commun.*, 997 (2000).
2. L. Xu, W.L. Zhuo, M.E. Kozlov, I.I. Khayrullin, I. Udod, A.A. Zakhidov, R.H. Baughman, and J.B. Wiley, *J. Am. Chem. Soc.* **123**, 763 (2001).
3. B.T. Holland, C.F. Blanford, and A. Stein, *Science* **281**, 538 (1998).
4. O.D. Velev, P.M. Tessier, A.M. Lenhoff, and E.W. Kaner, *Nature* **401**, 548 (1999).
5. S.A. Johnson, P.J. Ollivier, and T.E. Mallouk, *Science* **283**, 963 (1999)
6. A.A. Zakhidov, R.H. Baughman, I.I. Khayrullin, I. Udod, M. Kozlov, N. Eradat, V. Z. Vardeny, M. Sigalas, and R. Biswas, *Synth, Metals* **116**, 419 (2001).
7. R. Rengarajan, P. Jiang, V. Colvin, and D. Mittleman, *Appl. Phys. Lett.* **77**, 3517 (2000).
8. (a) N.D. Deniskina, D.V. Kalinin, and L.K. Kazantseva, *Gem Quality Opals: Synthetic and Nature Genesis*, Nauka, Novosibirsk, 1988 (in Russian); A.P. Philips, *J. Mater. Sci. Lett.* **8**, 1371; and (c) P.J. Darragh, A.J. Gaskin, and J.V. Sanders, *Scient. Amer.* **234**, 84 (1976).
9. C.F. Blanford, H. Yan, R.C. Schrodin, M. Al-Daous, and A. Stein, *Advanced Materials* **13**, 401 (2001).
10. H. Yan, C.F. Blanford, B.T. Holland, M. Parent, W.H. Smyrl, and A. Stein, *Advanced Materials* **11**, 751 (1999).